RZ 3432 (# 93713) 07/22/02
Electrical Engineering 14 pages

# Research Report

## Tracking in the Millipede System

H. Pozidis, E. Eleftheriou and G. Binnig

IBM Research
Zurich Research Laboratory
8803 Rüschlikon
Switzerland

# Tracking in the Millipede system

H. Pozidis, E. Eleftheriou and G. Binnig
*IBM Research, Zurich Research Laboratory, 8803 Rüschlikon, Switzerland*

**Abstract**

This note sketches several approaches for tracking in the Millipede system. Emphasis is placed on position error signal (PES) generation because this is the starting point and most critical component of any tracking servo system. The peculiarities of the Millipede and the possibilities it offers for tracking are outlined, and several ways to exploit them are proposed.

# 1 Introduction

The Millipede, a new AFM-based data storage concept, promises ultra high storage densities, small form factors and high data rates [1]. According to the latest demonstrations, bits with a diameter of 30-40 nm have been 'written' by a single cantilever/tip in a thin PMMA layer, resulting in a data storage density of 400-500 Gb/in$^2$. Owing to limitations in the scanning speed of a single cantilever, massive parallelization is needed to achieve high data rates. Towards this end, dense arrays of $32 \times 32$ cantilevers with integrated write/read functionality were built. Writing and reading are performed by time-multiplexing the electronic signals that control the access of the cantilevers in one row or column of the 2-D array.

With bits so densely spaced as in the Millipede, accurate tracking becomes a critical issue. Tracking means controlling the position of each tip, such that it is always positioned over the center of each written track during reading. During writing, the tip position should be such that the written bits are aligned in a predefined way. In electro-mechanical systems, tracking is performed in a servo loop, which is driven by an appropriate error signal. Ideally, the magnitude of this error signal is a direct estimate of the vertical (cross-track) distance of the tip from the track centerline, and its polarity indicates the direction of this offset.

Position error signal (PES) generation for AFM-based storage devices has been investigated before, and a number of approaches exist [2]. However, based on the results reported, none of the previously proposed methods can achieve the tracking accuracy required for the Millipede system. It is the purpose of this note to summarize and, where necessary, identify the main requirements for tracking in the Millipede, with emphasis on PES generation. A few tracking servo formats are closely investigated and their merits and drawbacks are discussed and quantified by simulations. Higher-level issues related to tracking are also identified and several possible solutions proposed.

# 2 PES generation

## 2.1 General requirements

The PES indicates the deviation of the sensing element from its ideal position on a track. The PES generation process is highly dependent on the storage system under consideration, and especially on the way that information readout is performed. Magnetic and optical recording are two instructive examples: in magnetic recording, tracking information takes the form of prerecorded magnetic transitions placed at radially adjusted *servo sectors* interspersed with data sectors. Information in servo sectors is usually divided into *servo bursts*, which are radially offset with respect to each other. As the recording head passes through a servo sector it senses variable amounts of signal from each burst, the relative strength of which indicates the cross-track position of the head. In optical recording, on the other hand, position information is continuously extracted during normal data readout. In read-only systems, the servo information carriers are the data carriers themselves (in the form of depressions, or pits, of the material), whereas in WORM (write once read many) and rewritable systems they are grooves (trenches) and/or lands, which are etched on the recording layer of the disc. This different configuration is due to the partitioning of the photo-detector, the light-sensing element in an optical disc, which essentially provides multiple observations of readout information in the form of multiple channels.

The quality of the PES directly affects the stability and robustness of the associated tracking loop. Desirable characteristics of the PES are listed below:

**Linearity/Invertibility:** The PES should be uniquely decodable, in the sense that each PES value should be mapped to a unique cross-track position. In view of decoding complexity, the ideal PES should be linearly proportional to the cross-track position for a band of width equal to the track pitch (TP) around the track centerline.

**Robustness:** The shape of the PES and the position of its zero-crossings should not be affected by disturbances such as noise during readout, timing inaccuracies, or other imperfections.

**Repeatability/Consistency:** The PES shape should be identical around all track centers. This requirement is usually met (see [3]).

For the purpose of illustration, Fig. 1 shows an ideal PES, where the numbers correspond to track centerlines. The in-phase signal is zero at track centers and is linear across a cross-track length corresponding to one track pitch (plus and minus one half of a track pitch around each track center). Therefore, position error is uniquely mapped, to within a track pitch, to a PES value, and the other way around. The usefulness of the quadrature PES becomes apparent from Fig. 2, which shows a PES curve as it typically appears in practice. The notable degradation is the flattening of the in-phase signal around track borderlines, where it achieves its minimum and maximum values. To ensure unique PES decoding at these positions, a quadrature signal is also generated. As the quadrature signal, which is by definition phase-shifted by $90^o$ with respect to the in-phase signal, has zero-crossings at track borderlines, it helps remove the position ambiguity in the in-phase signal. This is achieved by using the in-phase signal around track centerlines and the quadrature signal elsewhere. The resultant PES signal is indicated by the bold lines in Fig. 2. It is piecewise linear, with constant (absolute) slope, at all cross-track positions. Although this example is taken from magnetic recording, the basic principle of in-phase and quadrature signals applies also in the Millipede case; the objective is the generation of a uniquely decodable PES.

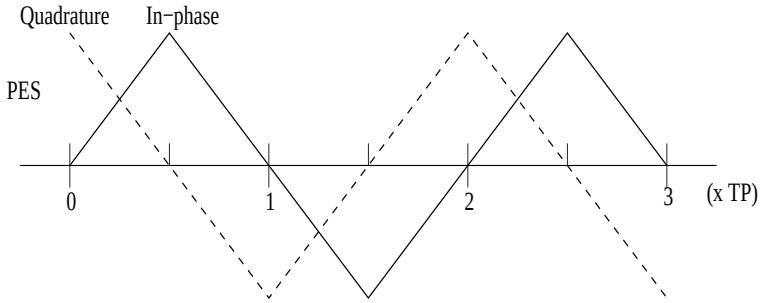


Figure 1: Ideal in-phase and quadrature PES.

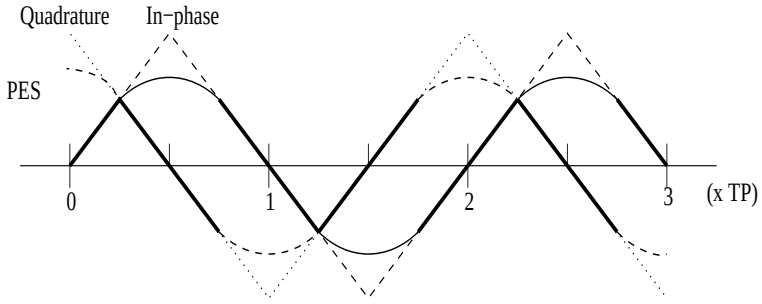


Figure 2: Typical in-phase and quadrature PES.

Although PES quality is important in its own right, special attention must be paid to the way it can be achieved, namely PES generation. Critical issues in PES generation are:

**Servo overhead:** The percentage of the storage area used for servo information should be kept as low as possible, because it reduces the area available for storing user information.

**Complexity:** This refers to both the time and effort it takes to create the servo patterns, as well as the delay/complexity of the demodulation process. Demodulation is the process of generating a PES, given a servo pattern. Overall complexity should be minimized for a cost-effective tracking system.

The readout mechanism of the Millipede system differs significantly from that of either magnetic or optical storage systems. As such, it calls for the development of different techniques for servo formatting and PES generation. Three such techniques are described below. First, a general overview of the Millipede system and the way data readout is performed is given.

## 2.2 Millipede system – data readout and placement

As stated above, the Millipede comprises an array of cantilevers. Each cantilever can write data to and read data from a dedicated area of a polymer substrate, called a *storage field*. In each storage field, data carriers take the form of polymer indentations; the presence of an indentation corresponds to a logical 1, and the absence of it to a logical 0. All indentations, also called *pits*, are nominally of equal depth and size, and are placed at a fixed horizontal distance from each other along a data track. We refer to this distance, measured from pit center to pit center, as the *bit pitch* (BP). The vertical (cross-track) distance between pit centers is also fixed, and is called the *track pitch* (TP). In order to read and write data the polymer medium is moved under the (stationary) cantilever array at a constant velocity. The scanning velocity determines the data rate of the system, in bits read or written per second. Based on this velocity one can translate units of distance to equivalent units of the time it takes to scan this distance. Hence we use time and distance interchangeably here. For example, BP nm (distance) corresponds to $T$ sec (time), where BP$= vT$, and $v$ is the scanning velocity in nm/sec.

Data readout is performed by monitoring the changes in temperature of the heated cantilever as it is scanned over tracks in a storage field. The cantilever temperature drops fast as the cantilever tip moves into a polymer indentation (pit), where the distance between heater and polymer is reduced, due to the more efficient heat transport through air. As pits do not have vertical walls in practice, they are modeled here as conical indentations of the medium. During motion of the polymer medium, the temperature change of a continuously heated cantilever is gradual as it moves from a pit edge down towards its center, where the pit depth is maximum. Although pits may not in reality be perfect cones, this model captures the main features of data readout while being mathematically tractable.

The cantilever is heated by a voltage (or current) source. For reasons of power conservation, periodic voltage pulses of short duration, rather than a DC voltage, are applied to the cantilever. During normal operation, one such pulse is fired every $T$ sec (corresponding to a distance of BP nm). The duration of the pulse is minimal compared to the time it takes to move in and out of the pit. Therefore, as the readout signal amplitude drops with the distance from the pit center, the timing of the system becomes critical. The effect of timing inaccuracies during reading on PES generation will be clarified below.

The impact of timing imperfections on the system can be reduced by oversampling. In effect, this means firing pulses more often than every $T$ sec. This improved robustness, however, comes at the price of higher power consumption, which might be prohibitive. To avoid this, one can apply oversampling only to a few selected cantilevers (and associated storage fields) as opposed to the entire array. The selected storage fields can be reserved exclusively for timing recovery and tracking purposes, two functions that can benefit from oversampling. Assuming that the number of such fields is small, this solution is advantageous in terms of overhead, compared to the alternative of timing and servo information embedded in all data fields (as is done in magnetic recording, for example). This is due to the large number of levers in the Millipede.

In the rest of this document we elaborate on the case of dedicated storage fields for storing servo information; these fields are called servo fields to differentiate from data fields, which store user information. The servo overhead, i.e., the ratio of the number of servo fields to the total number of fields, is a system parameter which determines the tradeoff between tracking servo performance and data storage capacity. We also impose the constraint that the readout of servo information must be performed in the same way as data readout, which simplifies the design of the system.

The following sections describe several proposals for formatting servo information in servo fields and placing these servo fields in the Millipede array.

## 2.3 Format of servo information

### 2.3.1 Servo pits

We describe here three alternative methods for PES generation. The three methods differ in the placement of servo pits in servo fields, giving rise to different PES curves. Generation of both in-phase and quadrature signals is described for reasons of unique PES decoding.

With the first method, which is referred to as scheme 1, servo pits are placed in bursts labeled $A$ and $B$ for the in-phase PES, and $C$ and $D$ for the quadrature PES. The centers of servo pits in burst $B$ are vertically offset by an amount equal to the pit diameter $d$ from pit centers in burst $A$. This ensures no overlap between pits in the two bursts. The same principle applies to pits in the quadrature bursts $C$ and $D$, with the additional condition that pit centers in burst $C$ are offset by $d/2$ from pit centers in $A$ in the cross-track direction. The latter condition is required in order to generate a quadrature PES, as will be explained below. The configuration of servo bursts in scheme 1 is illustrated in Fig. 3 for the case where TP=$3d/2$. Although each burst typically consists of many pits, to enable averaging of the corresponding readout signals, only two pits per burst are shown here to simplify presentation. The solid horizontal lines depict track centerlines whereas circles represent pits, which are modeled as perfect conical indentations of the polymer storage surface.

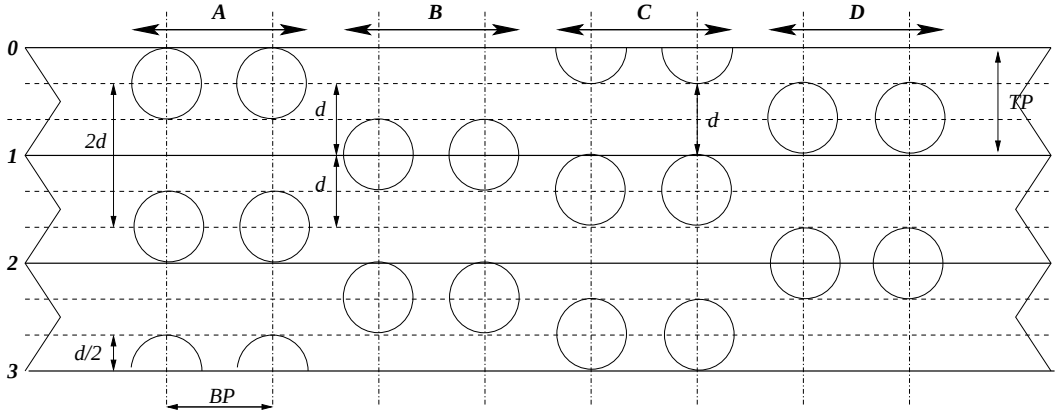


Figure 3: Servo burst configuration according to scheme 1.

To illustrate PES generation let us assume that pits in all bursts are spaced BP nm apart in the longitudinal direction, and that sampling occurs exactly at pit centers, so that timing is perfect. Let us further assume that the cantilever tip is located on the line labeled '0' and moves vertically towards line '3', in a line which crosses the centers of pits in burst $A$ (shown as dash-dotted lines in Fig. 3).[1] The tip moves from the edge of the top pit towards its center, then towards its bottom edge, then to blank space, then again to a pit, and so on. The readout signal magnitude decreases linearly with the distance from the pit center and is zero (or equal to a constant, background level) at a distance greater than the pit radius from the pit center according to the adopted (conical pit) model. To generate the in-phase signal, the tip is (conceptually) moved over burst $B$ and the readout signal is measured in a vertical line crossing the pit centers of $B$ (dash-dotted lines in Fig. 3). The in-phase signal is then generated as the difference $\bar{A}-\bar{B}$, where $\bar{A}$ and $\bar{B}$ stand for the demodulated signal amplitudes in bursts $A$ and $B$, respectively. This signal is represented by the line labeled 'I' in the top part of Fig. 6. It has zero-crossings at multiples of $d$, which do not generally correspond to track centers because we have set TP=$3d/2$. Therefore, the I-signal is not a valid PES in itself. This is where the quadrature (Q) signal becomes necessary. The Q-signal is generated from the servo readout signals from bursts $C$ and $D$, as $\bar{C}-\bar{D}$, and is also shown

[1]The vertical cantilever movement (actually the medium movement under the cantilever) is only conceptual because the actual movement is in the longitudinal direction, that is, parallel to the tracks. Vertical movement is only assumed here in order to illustrate the formation of the entire PES curve, that is, the curve arising by joining all PES values, where each value corresponds to a certain cross-track position of the cantilever.

in Fig. 6 (Q-curve). Note that it exhibits zero-crossings at points where the I-signal has local extrema.

A certain combination of the two signals (I and Q), shown in solid lines in Fig. 6, has zero-crossings at all track center locations and constant (absolute) slope, which qualifies it as a valid PES. However, this PES exhibits zero-crossings at all multiples of $d/2$. For the present example of TP=$3d/2$, three such zero-crossings exist at an area of width equal to TP around any track centerline. This fact, however, does not hamper unique position decoding. At even-numbered tracks, it is the zero of the *in-phase* signal that signifies the track center. The zeros of the quadrature signal, in turn, can be uniquely mapped into a position estimate by examining the polarity of the in-phase signal at the corresponding positions. This holds for any value of the combined PES within the area of width equal to TP around the current track centerline. The signals change roles for odd-numbered tracks. The track number, which is known a priori from the seek operation, is used to determine the mode of operation for the position demodulation procedure, given the PES value at hand. One limitation of scheme 1 is that, because it exhibits, by construction, zeros every $d/2$ space units, it effectively requires TP to be a multiple of $d/2$ in order for zero-crossings to occur at track centerlines.

The configuration of servo bursts in scheme 2 is illustrated in Fig. 4, also for the case TP=$3d/2$. The pits in each burst are now placed TP units apart vertically, whereas pit centers in bursts $A, B$ and $C, D$ overlap in the cross-track direction. The vertical distance between pit centers in burst $A$ and pit centers in burst $B$ alternates between TP $- d$ and $d$, as shown in Fig. 4, giving rise to an asymmetric PES. The idea behind scheme 2 is to generate an in-phase signal with zero-crossings at each track centerline, regardless of the values of TP and $d$. However, undesirable zero-crossings are also generated midway through each track. A quadrature signal is needed to resolve the ambiguity. As the quadrature signal has a phase difference of $2\pi/4$ radians from the in-phase signal by definition, pit centers in burst $C$ must be offset by TP$/4$ units from pit centers in burst $A$ in the cross-track direction. The I and Q signals for scheme 2 are shown in the lower part of Fig. 6. Although the I-signal is (piecewise) linear, it exhibits an asymmetry about its extrema, which arises from the asymmetric (vertical) placement of pits in bursts $A$ and $B$. As a result, zero-crossings of the I-signal do not align with extrema of the Q-signal and the opposite. As a result, unique decoding for scheme 2 tends to be more complicated compared to scheme 1.

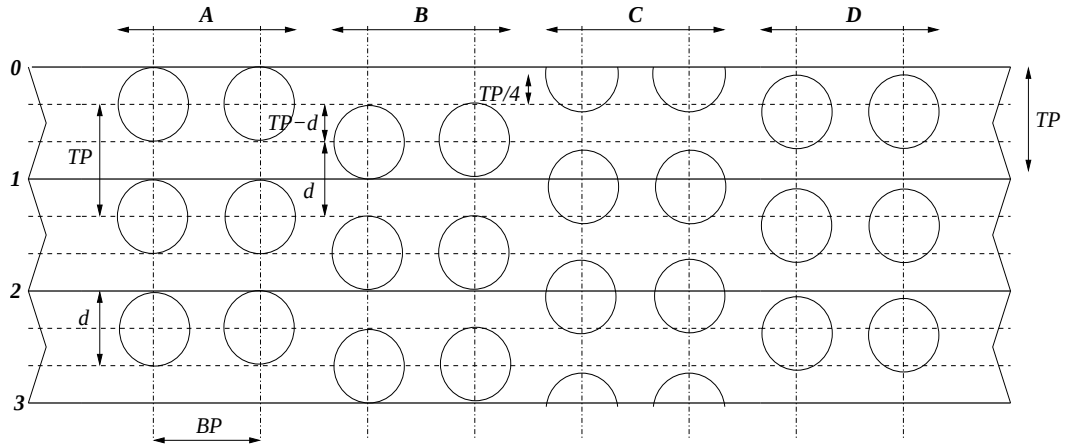


Figure 4: Servo burst configuration according to scheme 2.

A third configuration of servo bursts, which combines the advantages of the previous two topologies and yet circumvents most of their drawbacks, is illustrated in Fig. 5 for the case TP=$3d/2$. Similar to scheme 2, the generated PES has zero-crossings at track centerlines and halfway between. However, the undesirable zero-crossings can be easily resolved by the quadrature signal, which now has minima at track centerlines and maxima halfway between (or the opposite). The alignment of the extrema of one signal with the zeros of the other is achieved by placing the pit centers in bursts $A$ and $B$ (and also in $C$ and $D$) at equal vertical distances from each other. The distance between pit centers of the same burst is equal to TP, whereas the distance between pits in $A$ and $B$ (or $C$ and $D$) bursts is TP/2. The vertical

distance between $A$ and $C$ pits is TP/4, similar to scheme 2. The demodulated PES for the configuration of Fig. 5 is shown in Fig. 7. Although the PES is not linear throughout half of its period, it is uniquely decodable at all points by use of both I and Q signals.

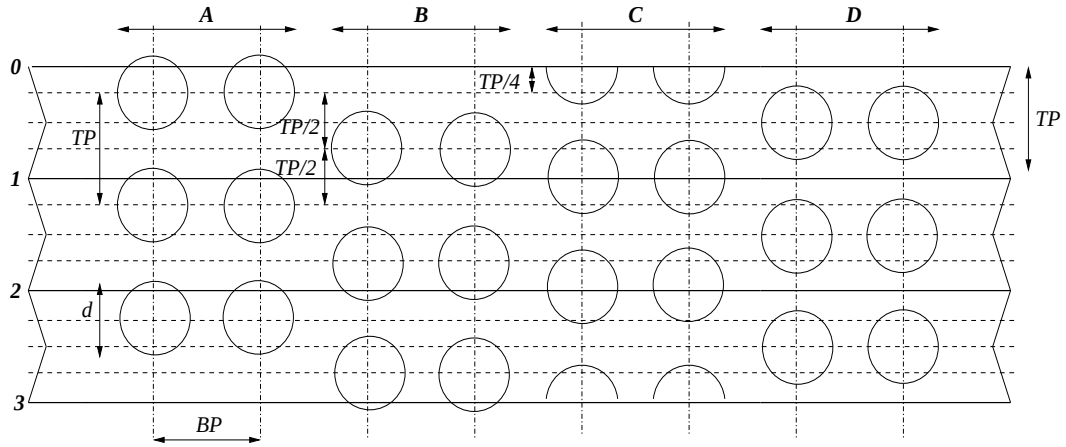


Figure 5: Servo burst configuration according to scheme 3.

The interesting property of scheme 3 is that it decouples the vertical distance of pits from the pit diameter $d$.[2] This is important because the pit diameter is variable and depends on parameters such as writing power. In practice it has been found that pits are not perfect conical indentations of the polymer medium, but instead exhibit rings around the indentation. This means that the diameter of the indentation is smaller than the pit diameter. PES demodulation, however, is based on the principle that the servo readout signal decreases in magnitude away from the tip center and reaches a background level at a distance equal to $d$ from the center. If the indentation diameter is reduced, the 'effective' range for PES demodulation also decreases. To ensure unique decoding and avoid multiple zero crossings, one can bring the $A$ and $B$ (and $C$ and $D$) bursts closer vertically, so that they overlap in the cross-track direction. Scheme 3 offers this flexibility, as shown in Fig. 5, in addition to maintaining unique decoding.

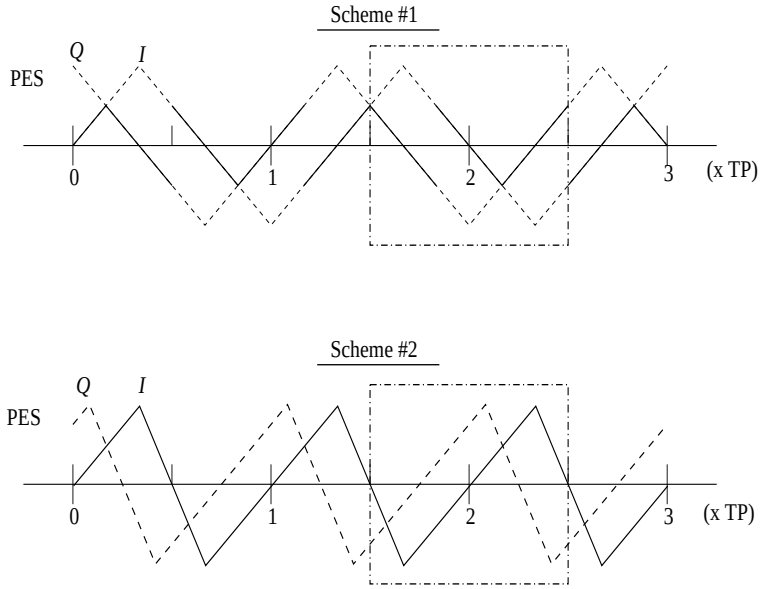


Figure 6: Ideal position error signal (PES) for schemes 1 and 2.

[2]This is also achieved by scheme 2, but at the expense of unique position decoding due to the asymmetric nature of the corresponding PES.

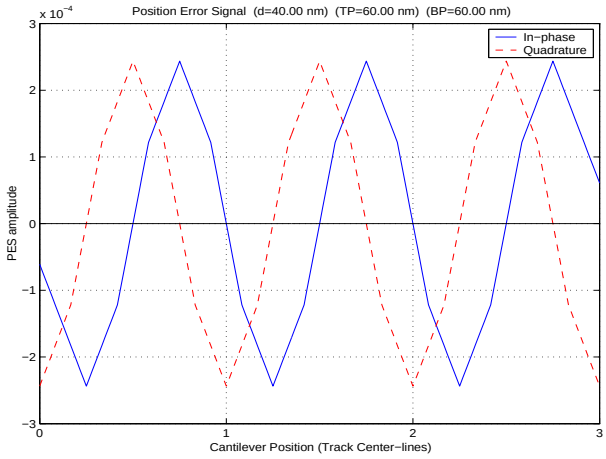


Figure 7: Ideal position error signal (PES) for scheme 3.

Other servo burst configurations are possible; the possibilities are virtually endless. However, the three schemes described above possess several desirable features. First, they are all easy to fabricate; in fact, the servo fields can be written by the cantilever itself because all schemes were designed based on the constraint that servo readout is performed in the same way as data readout. Therefore, a servo field resembles a data field, the only difference being (possibly) in the vertical placement of pits. Self-writing is significantly cheaper and faster than, for example, etching of servo information, which involves lithography. A second, related advantage is that servo demodulation is almost identical to data readout. Specifically, a pulse of short duration is fired when the cantilever tip crosses a (virtual) vertical line connecting pit centers (the location of which is determined by the timing loop), and the resulting change in temperature is sampled and held at the position of maximum amplitude (a form of peak detection). This means that any cantilever can be used for PES generation, thus simplifying the design of the system electronics.

### 2.3.2 Servo Grooves

The servo burst formats discussed in the previous subsection are based on pits, and as such the servo readout signal is sensitive to timing errors. Timing errors cause sampling errors, that is, the read pulses are fired at times that do not accurately correspond to pit centers. Thus, even when the tip is positioned exactly on the track centerline, the readout amplitude does not achieve its maximum value because the pit center is 'missed'. This leads to loss of amplitude for the demodulated PES at its local extrema, and to flattening around its zero crossings. This phenomenon is also verified in the simulations section that follows.

One way to improve the robustness of the PES to timing variations would be to make elongated indentations, that is, indentations that are longer in the longitudinal direction. In the limit, the gaps between pits within a burst are 'filled', thus creating only one (or several) 'fat' pit per burst, which covers the entire track length previously occupied by several pits. These elongated pits are then trenches or grooves along a prespecified length of the track. The concept is illustrated in Fig. 8, which is a modification of scheme 1 in Fig. 3, with servo grooves in place of servo pits. The parameters of scheme 1 do not change. Schemes 2 and 3 can be modified in a similar way. As argued above, the main advantage of servo grooves is their robustness to timing errors. This can be seen in Fig. 8: even if sampling does not occur at times corresponding to the dash-dotted vertical lines (which virtually connect pit centers in Fig. 3), the PES signal will not be affected because the indentation of the polymer along the cross-track direction is now continuously present longitudinally.

The advantages of the servo burst configurations discussed in the previous subsection carry over to servo grooves; self-writing of servo information is still feasible, whereas servo demodulation is identical

to the servo pits case. One possible drawback of servo grooves is that they may require higher power for writing compared to servo pits. However, as servo information is only written once, this issue tends to be of minimal importance.

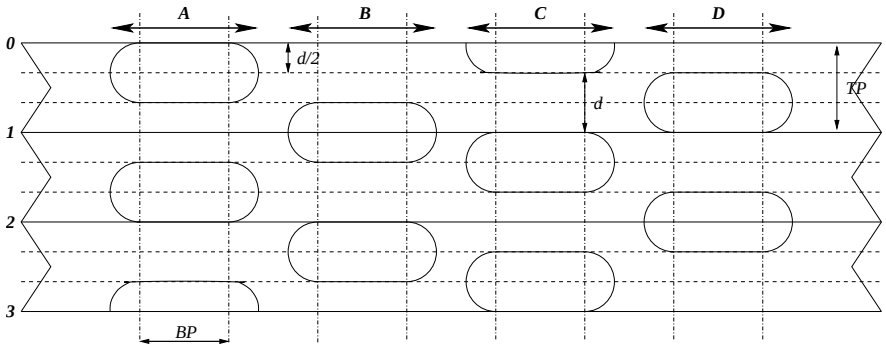


Figure 8: Servo burst configuration similar to scheme 1 with grooves instead of pits.

## 2.4 Simulations setup for PES generation and results

The quality of the PES signals generated by the schemes described above is tested here by simulations. The simulation program generates a sequence of four servo bursts, each consisting of a variable (but equal for each burst) number of servo pits. The pit diameter $d$, track pitch and bit pitch are program parameters, and determine the shape of the resulting PES. In practice, readout is performed by firing electrical pulses of short duration while moving the polymer surface under the tip. The amplitude of the readout signal depends on the position of the tip relative to the recorded surface when a pulse is fired. The readout signal is strongest when the tip is positioned exactly over the center of a pit at the time a pulse is fired. As the distance of the tip from the pit center increases, the readout signal strength decreases, reaching a constant background level when the tip is away from a pit indentation. To simulate this characteristic, pits are modeled as conical indentations of the polymer storage medium. This means in effect that the readout signal strength decreases linearly with the distance from the pit center, and reaches the background level when this distance exceeds the pit radius.

The simulated readout signal is generated as a superposition of readout pulses, which are amplitude modulated by the *pulse position sequence.* This is a sequence of real values from $[0, 1]$, which characterize the position of the tip relative to the closest pit center, at the pulse firing moments. The readout pulse response of the system is generated by a separate simulation that takes into account the electrical characteristics of the cantilever. In mathematical terms, the readout signal can be written:

$$r(t) = \sum_{i=-\infty}^{\infty} a_i p(t - \tau_i), \tag{1}$$

where $a_i$ stands for the pulse position sequence, $p(t)$ is the readout pulse response of the cantilever, and $\tau_i$ are the pulse firing instances. Denoting the pit radius by $R$, the pulse position sequence is given by

$$a_i = \begin{cases} \frac{R-d_i}{R}, & \text{if } d_i \leq R \\ 0, & \text{otherwise} \end{cases} \tag{2}$$

where $d_i = ((x_i - x_0)^2 + (y_i - y_0)^2)^{1/2}$ is the Euclidean distance between the tip position $(x_i, y_i)$ at the pulse firing moment and the center $(x_0, y_0)$ of the closest (in Euclidean distance) pit indentation. In the nominal situation, i.e., when the tip is on track $(y_i = y_0)$ and the pulse is fired when the tip is exactly over the pit center $(x_i = x_0)$, we get $d_i = 0$ and $a_i = 1$, the maximum value of the readout signal amplitude.

This model has two degrees of freedom, which provides the flexibility needed for PES generation. The first is the vertical, or cross-track, position of the tip relative to the servo pit centers. Variation of this position directly affects the readout signal amplitude, which can then be used to yield a PES value. The second parameter is the horizontal distance of the tip from the servo pit centers. By varying this distance one can study the effects of inaccurate timing on the PES. Inaccurate timing leads to firing electrical readout pulses at instances not aligned with written information, causing a deterioration of the readout signal. Even when the tip is on a track centerline, errors in timing cause a non-zero PES, which can lead to false position locking if these errors are consistent, for example in the form of constant phase offsets. In practice, however, a timing loop will eliminate constant frequency and phase offsets, leaving only random timing fluctuations uncompensated. The effect of these random timing fluctuations, or timing jitter, on the position error signal will be examined below.

Two sources of disturbances are included in the simulation of servo data readout. The first is Gaussian white noise, which is added to the servo readout signal at a certain signal-to-noise ratio (SNR). It is defined as SNR $= 20\log_{10}(V_s/2\sigma_n)$, where $V_s$ is the maximum peak-to-peak amplitude of the readout pulse when it is fired exactly when the tip is over a pit center, and $\sigma_n$ is the standard deviation of the noise process. The second disturbance is timing jitter, which causes pulse firing instances to deviate from their nominal positions corresponding to pit centers. Letting $t_i = iT$ be the nominal firing moments, jitter $\Delta t_i$ is modeled as a noise process (with Gaussian or uniform distribution) which is added to $t_i$, giving the actual pulse firing instances $\tau_i = iT + \Delta t_i$.

For PES generation, the readout signal from each servo burst is sampled synchronously with the pulse firing instances at the point where the readout pulse attains its maximum amplitude, and the sampled values are averaged within a burst. The average values $\bar{A}, \bar{B}, \bar{C}$ and $\bar{D}$, corresponding to bursts $A, B, C, D$, are then used to calculate the PES value at each cross-track position of the tip, as $\bar{A} - \bar{B}$ and $\bar{C} - \bar{D}$ for the in-phase and quadrature signals, respectively. For the purpose of illustration, Fig. 9 shows a simulated PES in the absence of noise and timing errors for the configuration of scheme 1. The pit diameter, track pitch and bit pitch are set to $d = 40$ nm, TP=60 nm and BP=60 nm, respectively, and each burst comprises eight servo pits. Both in-phase and quadrature signals are shown. As expected, the PES amplitude, the zero-crossing positions and the slope are all distorted in the presence of noise and/or timing inaccuracies. The effect of noise on the PES is shown in Fig. 10, for SNR=10 dB. Figure 11, in turn, shows the demodulated PES in the presence of timing jitter, with a standard deviation equal to 10% of the bit period $T$. Finally, the combined effects of noise and timing jitter are shown in Fig. 12. Although noise causes variations of the PES around its nominal shape, it does not affect the PES amplitude nor its slope around zero crossings. On the other hand, timing jitter decreases both amplitude and slope of the PES, and thus it can potentially hamper unique position decoding.

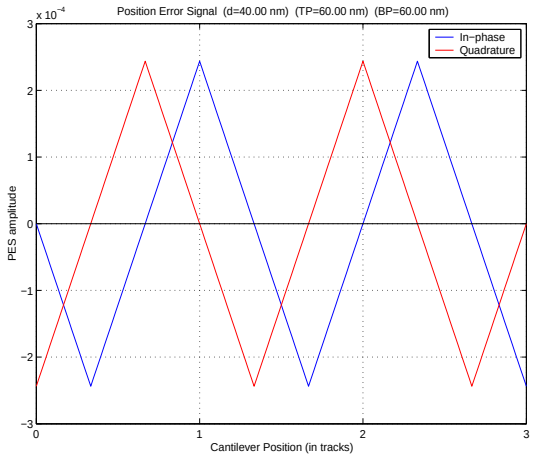


Figure 9: In-phase and quadrature PES in the absence of noise and timing errors.

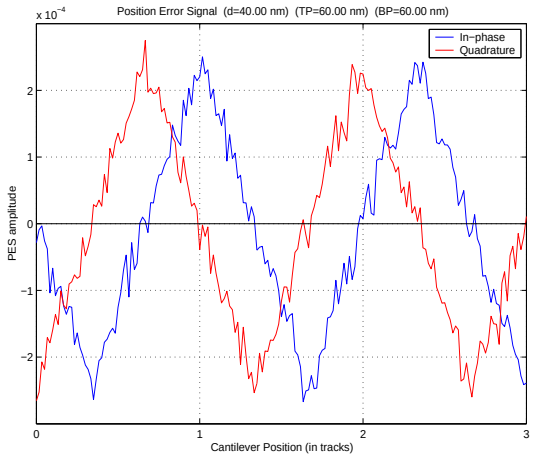


Figure 10: In-phase and quadrature PES in the presence of noise.

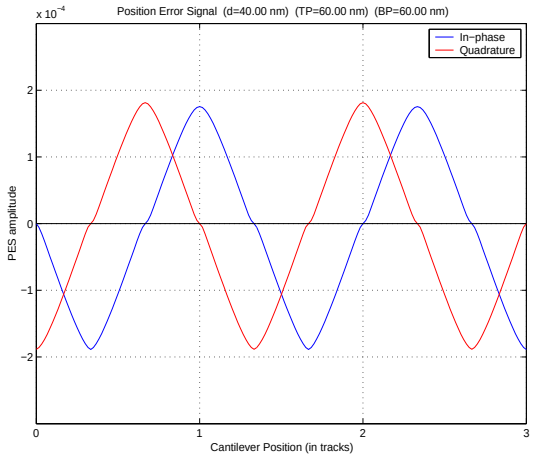


Figure 11: In-phase and quadrature PES in the presence of timing jitter.

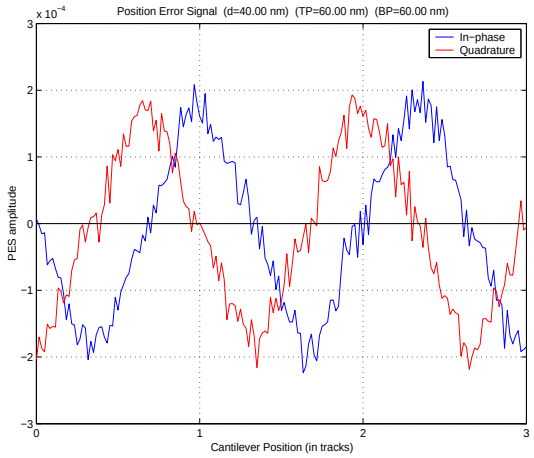


Figure 12: In-phase and quadrature PES in the presence of noise and timing jitter.

The quality of a PES signal and its robustness to varying amounts of disturbances are commonly quantified by two measures: the position accuracy of the PES zero-crossings at track centerlines, and the slope of the PES at and around these zero-crossings. The zero-crossing accuracy is critical because any deviation from the nominal position can lead to track misregistration (TMR), that is, a deviation of the decoded tip position from the actual position of the track center during track following. The slope of the PES, in turn, serves as an indication of the uniqueness of position decoding: small slopes indicate nearly flat areas, which may lead to uncertainties in PES decoding.

Figure 13 shows average slope at and around the zero-crossings of the PES with varying degrees of jitter for two of the servo schemes described (similar results are obtained for scheme 3). Jitter variance is shown as a percentage of the bit period $T$, and the slope as a percentage of the nominal slope in the absence of jitter. It is apparent from the graph that timing jitter mainly affects the slope of the PES exactly at its zero crossings, leading to an uncertainty about the tip position around track centerlines. This holds for both schemes considered, and stresses the significance of accurate timing for reliable operation of the tracking servo loop.

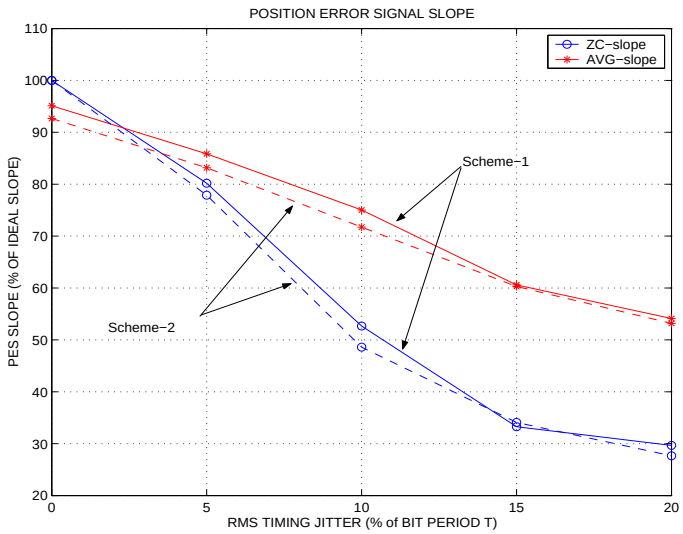


Figure 13: PES slope degradation for schemes 1 and 2 in the presence of timing jitter. ZC-slope stands for the average slope exactly at the PES zero-crossings, and AVG-slope is the average slope around the PES zero-crossings.

Figure 14 shows average offset (in nm) from the nominal zero-crossing positions of the PES (of scheme 1) for varying noise conditions. The two curves correspond to bursts of 4 and 8 pits, respectively. As expected, more averaging helps reduce the noise effects on the PES, although the absolute zero-crossing offset is minimal even at extreme noise conditions (the sub-nm offset is a small fraction of the pit diameter, which is set to 40 nm in the example shawn). Each point in the curves is the result of averaging over 50 different realizations of either jitter or noise sequences.

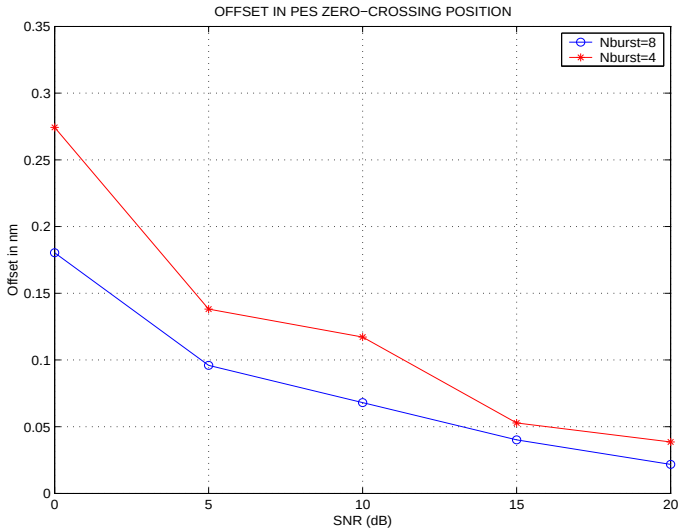


Figure 14: Zero-crossing position offset for scheme 1 in the presence of AWGN.

The simulation results indicate that it is mainly timing jitter and not noise that affects the quality of the PES, provided that adequate averaging is performed in the demodulated servo readout signal. This effect can be reduced by oversampling. By firing more pulses per bit interval, timing uncertainty, and thus jitter, can be minimized. This, of course, has to be traded off against an increase in power consumption, as stated above.

# 3 Experimental results on PES generation

The principle of PES generation based on servo pits has also been verified experimentally. Towards this end, $A, B, C, D$ bursts according to scheme 1 have been written by an AFM cantilever/tip on a polymer medium consisting of a 130 nm SU-8 coating on top of a silicon substrate. The bit pitch was set to 42 nm and the track pitch was taken to be approximately equal to $d$, the pit diameter. An image created by reading the written pattern with the same cantilever is shown in Fig. 15. Shaded areas indicate pit indentations.

The readout signal from the cantilever was also used for servo demodulation, as described in the previous sections. The resulting in-phase and quadrature PES are shown in Fig. 16. The track centerlines are indicated with vertical dotted lines in the graph. It can be observed that the zero crossings of the in-phase signal are closely aligned with the track centerlines, and that the PES slope is nearly linear along a cross-track width of one track pitch around each track center (since $TP \approx d$). Moreover, the zero crossings of the quadrature signal are aligned with the minima and maxima of the in-phase signal, thus enabling unique position decoding even at flat areas of the in-phase signal. Although these results are preliminary and the read/write process is not yet optimized, the experimentally generated PES signals show that the proposed tracking concept is valid and promising. Specifically, the results indicate that servo self-writing is feasible, that servo demodulation is almost identical to data reading and can be performed by any lever without special provisions, and that the resulting PES possesses the desirable features described previously.

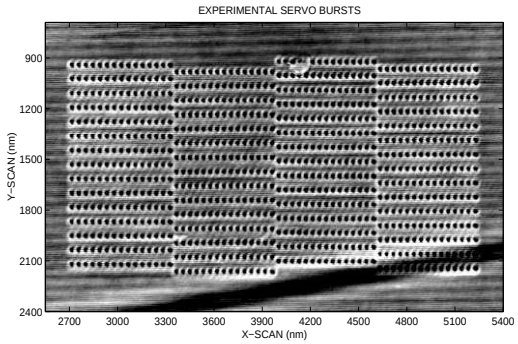


Figure 15: $A, B, C, D$ servo bursts (scheme 1) written by a single cantilever on a 130-nm-thick SU-8 polymer medium. The track pitch and bit pitch are set to 84 nm.

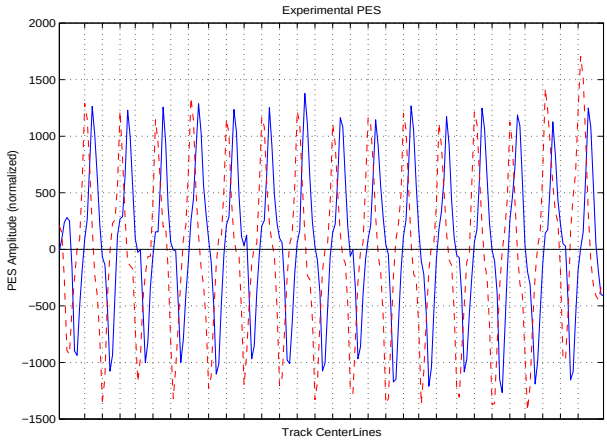


Figure 16: Demodulated in-phase and quadrature PES based on the servo bursts of Fig. 15.

# 4 Distribution and placement of servo fields

In this section we discuss the issue of allocating storage fields as dedicated servo fields within the Millipede field array. In practice, an overhead budget is commonly assigned, which determines the maximum allowable number of servo fields in the array. Placement of these servo fields is then a degree of freedom that can be exploited to enhance the robustness of the tracking subsystem to various disturbances. This is a unique feature of the Millipede, being an array-based storage system that enables parallel access of multiple storage fields.

We initially assume that a fixed servo overhead budget has been assigned and proceed to discuss servo field placement. Some of the factors that have an impact on field placement are listed below.

**Parallelism:** Parallel access of multiple fields along (at least) one dimension of the Millipede array enables instant collection of an amount of written information which can be exploited for various purposes. By placing a number of servo fields along the parallel-accessed dimension (say a row of the array), one can either instantly generate PES samples, or collect several samples from a servo burst at once. For example, assume that four servo fields are placed in some row of the array and number them 1 to 4. One option then is to write bits of only one servo burst in each of the four fields; the first field contains only bits of burst $A$, the second of burst $B$, and so on. Then, each time the row is read, one sample from each burst is obtained, thus one PES sample is generated. In another configuration, all four fields are similar, each containing pits of all four bursts. During readout, four samples of the same burst are obtained at once, enabling averaging to take place.

The first topology is advantageous in terms of frequency of generation of PES samples, which is important in situations where the scanner position drifts rapidly, causing tracking errors. However, as only one PES sample is obtained (in the specific example), instantaneous distortion and noise can hamper the quality of the sample. The second arrangement, on the contrary, leads to more reliable servo burst samples, but requires more time to generate a single PES sample. Of course other topologies, offering various degrees of reliability versus PES sample rate are possible. The choice of one solution over the others depends on the characteristics of the system, the nature and severity of disturbances (e.g. shocks), and the scanner movement, among other factors.

**Redundancy:** In the case of a system like Millipede, redundancy in principle amounts to repeating similar information in several spatially separated areas of the storage medium in order to enhance robustness to disturbances or various operating conditions (e.g. shocks). It is an integral feature of nearly every tracking servo format. Redundancy manifests itself on two levels: on the fine level, it amounts to repeating the same information within a servo burst to enable the effects of

random errors, e.g. due to noise, to be averaged out. On the coarse level, entire servo information areas may be duplicated in spatially distinct areas of the medium, with a dual purpose; first, to generate position error information at a sufficient frequency (high PES sample rate), and second, to provide alternative information in case burst errors destroy (either partly or entirely) one or more servo areas. Burst errors are typically caused by scratches, media defects, or other media-dependent imperfections. Moreover, in a contact recording system such as the Millipede, the tips can potentially damage the recording surface, or the tips themselves can be damaged, so additional protection will probably be necessary.

**Medium motion:** In the Millipede, the storage medium is placed on top of a scanner, which moves it in the $X$ and $Y$ directions. The mechanics of this motion are of special importance for servo placement. They determine, for example, the minimum frequency of occurrence of servo data in order to maintain the tips on track during motion of the medium. Moreover, if, for example, the medium moves at a certain angle with respect to the tip array, servo field placement can serve to monitor dynamic changes of this angle during system operation.

The possibilities for servo field placement in an array of fields is a subject requiring careful consideration of all relevant parameters, including the ones described above. Instead of listing several possibilities, which would not be instructive, we discuss only three of them to illustrate the main characteristics. First we assume, without loss of generality, that the array comprises $32 \times 32$ storage fields and assign 16 of them as servo fields, an overhead of 1.6%. We also assume that all fields in rows of the array are accessed in parallel.

Figures 17, 18 and 19 illustrate three possible servo field arrangements. The 16 servo fields are indicated by shaded squares. In the first topology, all 16 servo fields are placed in the first row of the array, giving the maximum possible amount of averaging for each servo burst sample. As all fields are accessed in parallel, it is advantageous to write only bits of one servo burst in each field; that is, the first four servo fields contain only $A$ burst bits, the next four have $B$ burst bits, and so on, with other arrangements being possible (such as $A$-$B$-$C$-$D$-$A$-...). This scheme will then generate 4 PES samples at one read access. However, as reading is done sequentially line-by-line, it will take $T_s$ seconds until the next PES samples are formed, where $T_s$ is the time required for a complete array scan. In the second topology, averaging is traded off for frequency of occurrence. Now two PES samples are formed at one access, but two more follow after $T_s/2$ seconds, to enable tracking of fast position variations. The third topology offers the maximum frequency of servo information occurrence, with one PES sample generated every $T_s/4$ seconds (each of the four fields in any row comprises only the bits of one burst, as in scheme 1). This, however, is done at the expense of increased susceptibility to noise and random errors due to the lack of instant averaging as in the other two schemes.

In addition to trading averaging for sample rate, one can also place fields in the array in order to achieve robustness to errors. All of these requirements can be satisfied, to a certain degree, concurrently. For example, suppose one expects that the failure probability of several fields and/or cantilevers that lie

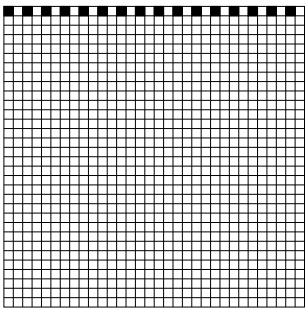

Figure 17: Placement of servo fields according to scheme 1.

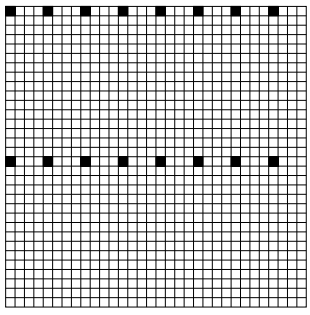

Figure 18: Placement of servo fields according to scheme 2.

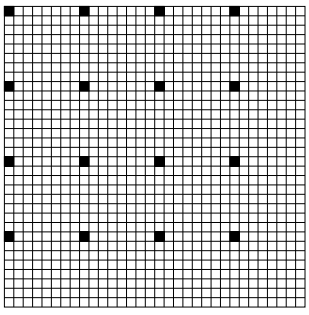

Figure 19: Placement of servo fields according to scheme 3.

in a column is higher than for other fields. In that case, one should avoid placing fields comprising bits of the same burst in one column. In particular, referring to scheme 3, it could be advantageous to have single-burst fields shift cyclically: place fields $A$-$B$-$C$-$D$ in the first row, then fields $B$-$C$-$D$-$A$ in the subsequent row, then $C$-$D$-$A$-$B$, and so on, so that even if one complete column of fields fails, then PES generation will still be possible from the remaining fields.

A very large number of different topologies can be conceived, some with possibly better properties than the ones sketched here. It must be stressed that this presentation is only meant as a guideline; the actual scheme choice is strongly dependent on the particular application, the actual parameter settings, the error sources and other factors.

# References


[1] P. Vettiger et. al., "The "Millipede" – More than one thousand tips for future AFM data storage", *IBM J. Res. Develop.*, vol. 44, no. 3, pp. 323-340, May 2000.

[2] H. J. Mamin, R. P. Ried, B. D. Terris, and D. Rugar, "High-Density Data Storage Based on the Atomic Force Microscope", *Proc. IEEE*, vol. 87, no. 6, pp. 1014-1027, June 1999.

[3] A. H. Sacks, *Position signal generation in magnetic disk drives*, Ph.D. Thesis, Carnegie Mellon University, 1995.